Lifelong 3D Mapping – Monitoring with a 3D Scanner

Dorit Borrmann, Jan Elseberg, Shaan S. Rauniyar, and Andreas Nüchter

***Abstract*— Geodesy and surveying are the sciences for monitoring the earth. In recent years traditional surveying equipment has been pushed aside by the emerging technology of laser scanners, that automate the precise measurement of points in the environment. A further step of automation is achieved by operating the surveying equipment automatically and the usage of robotic mapping. Thus, robotic mapping will become a key component in monitoring and surveillance tasks. This paper evaluates a 3D laser scanner from surveying for its usage in robotic monitoring tasks. We examine how seasonal changes and weather conditions impact the data of the 3D scanner and how to deal with these changes. For this analysis 3D scans of various predetermined locations on the campus of the Jacobs University Bremen were taken on a weekly basis over a period of 13 weeks using the RIEGL VZ-400 3D laser range finder. The scans have been registered by means of conventional surveying markers, SIFT features and using our point cloud based 6D SLAM framework. An analysis of the changes in the environment over the course of the scanning period and an evaluation of the matching results complete the analysis.**

I. INTRODUCTION

As mobile robots move out of laboratories they often face non-static environments. These environments can be classified according to the speed of change. On one hand, dynamic environments usually refer to fast changing environments, e.g., populated work spaces. Also driver assistance or traffic and factory monitoring systems fall into this category, since the algorithms have to cope with fast changing worlds. On the other hand, there are many things that change slowly, e.g., construction sites change gradually demonstrated by the fact that some historic buildings show even different architectural styles, or vegetation changes slowly as trees grow, flowers bloom, etc. Seasonal changes fall into the category of slow changes, too.

For many applications in environmental monitoring large areas need to be monitored over long time periods. If a robot is applied for monitoring such an area the time periods between two encounters of the same location will also be long. While gradual changes appear regularly over the course of a year, small changes often mark the beginning of upcoming severe conditions such as landslides or levee breakages. Therefore it is necessary to create precise maps of the environment in spite of temporal changes and regardless of changing weather conditions in the partial maps. In this paper we evaluate the applicability of laser scanning technologies for this task. We analyze laser data acquired at different weather conditions including gradual seasonal changes and evaluate different mapping procedures.

The authors are with the Automation Group at the School of Engineering and Science, Jacobs University Bremen gGmbH, 28759 Bremen, Germany {d.borrmann|j.elseberg|s.rauniyar|a.nuechter}@jacobs-university.de

Fig. 1: The Riegl VZ-400 3D laser scanner mounted on a tripod and a self assembled dolly. The scanner has manually moved to different positions as the campus of Jacobs University Bremen.

Changing environments impose several challenges for robots as the robot control relies on sensor values. In navigation tasks, landmarks must be reliably recognized. In robotic mapping, consistent representations have to be generated with regard to the changes. Automatic monitoring algorithms must be able to abstract and to detect *important* changes, which are –of course– application dependent.

The availability of cost effective safety laser scanners from industrial automation for mobile robots has revolutionized mobile robotics in recent years. Well known manufacturers of such devices are SICK, Schmersal, Leutze, and Hokuyo. Besides these pulsed laser scanners, high-end devices for surveying applications exists. These scanners work either with continuous light waves or laser pulses. Aerial Light Detection and Ranging (LiDAR) has been used for over a decade to acquire highly reliable and accurate measurements of the earth's surface [3]. Terrestrial LiDAR systems such as the one presented in Fig. 1 are used for example in as-built documentation of industrial plants and ship-building. These systems have left pre-commercial development and have reached the state of technically mature systems. Unlike several years ago, terrestrial LiDAR systems are made available from a number of vendors. However, they are lacking formal standardization of accuracy evaluation and testing as specific tests show [17], [16]. Typically, the software, workflow and final products in terrestrial LiDAR are rather application-specific. When paired with classical surveying, terrestrial LiDAR delivers highly accurate and referenced geo-data.

A general review of range sensor systems is given in [5] including triangulation and LiDAR systems. State of the art in terrestrial large volume data acquisition is the use of high

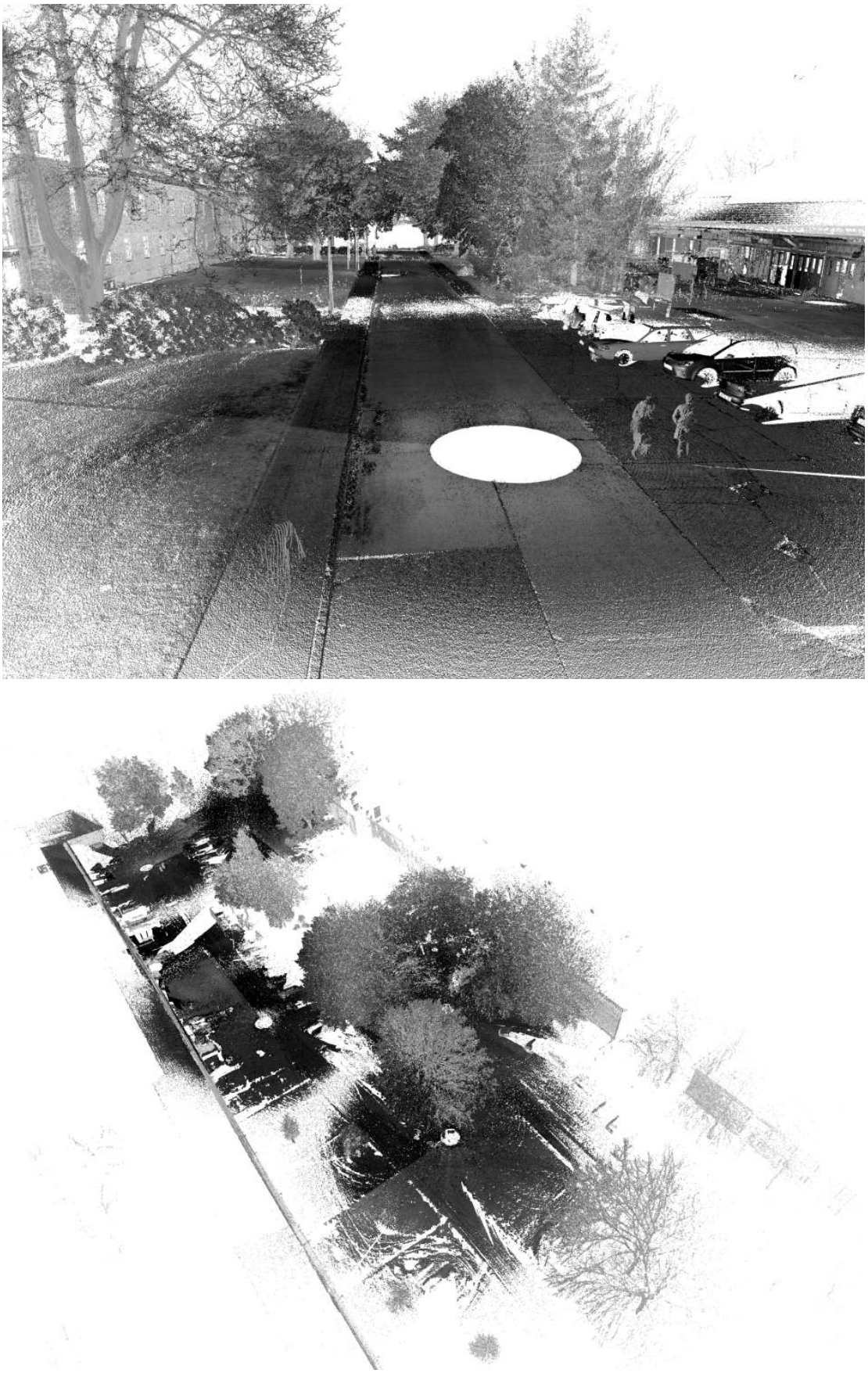

Fig. 2: 3D scene as a point cloud. Top: Street view. Bottom: Bird-eyes view.

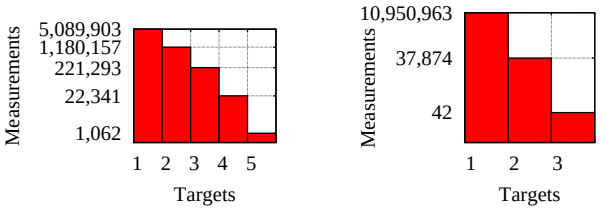

Fig. 3: Histogram of the number of echoes detected by the online full wave analysis of the VZ-400 scanner. Top: Scan mode "high-speed" (week 1). Bottom: Scan mode "high-speed reflector scanning" (week 2).

resolution LiDAR systems. These sensors emit a focused laser beam in a certain direction and determine the distance to an object by measuring the reflected light. The distance to an object surface can be calculated from the time difference between the emitted and measured signal. This technology makes the sensors independent from external light, e.g., daylight.

Our long-term objective is to automate terrestrial LiDAR systems and to use these systems for inspection and monitoring. To this end, this paper evaluates the data of such a device over a long period of time and presents initial results for mapping and monitoring applications. Inspired by the seminal work about "SIFT, SURF and Seasons: Long-term Outdoor Localization Using Local Features" by Valgren and Lilienthal [15] we aim at investigating and analyzing changes that happen in an environment over a large period of time. In this paper, we analyze the performance of mapping algorithms in different seasons and present monitoring results on basis of our mapping framework 6D SLAM [1].

The remainder of this paper is structured as follows: Next, we describe the used laser scanner that comes with a commercial software package. Figures with black background in this paper have been produced with this software package while images from the viewer in 6D SLAM have white background. Section III describes briefly the used mapping algorithms and presents the result of our study. After mapping, we describe the findings for monitoring. Section V concludes.

II. DATA ACQUISITION

A. The RIEGL VZ-400 3D Laser Scanner

In our experiments, we use the RIEGL VZ-400 3D laser scanner manufactured by Riegl Laser Measurements GmbH, Austria [14]. This V-Line 3D terrestrial laser scanner provides high speed, non-contact data acquisition using a narrow infrared laser beam and a fast scanning mechanism (cf. Fig. 1). The line scanning mechanism is based upon a fast rotating multi-facet polygonal mirror, which provides fully linear, unidirectional and parallel scan lines. The line scanning device is rotated around the vertical axis to yield a field of view of 100° (-40° to +60°) × 360°. According to the data sheet the maximum scanning range is up to around 350 meter at average and the measurement rate is 125.000 points per second. Its accuracy defined as the degree of conformity of the measured quantity to its actual (true) value, is 5 mm and the precision, i.e., the reproducibility or repeatability, defined as the degree to which further measurements show the same results, is specified as 3 mm.

The scanner returns range measurements. In addition to every range measurement, the amplitude and remission, i.e., the amount of light that is returned to the scanner, is quantified. The weight of the scanner is 9.8 kg and it is dust and splat proof (protection class IP 64). As an eye-safe class 1, shock-proof, laser scanner with a typical power consumption of 65 W it should be a well suited robot sensor.

B. Scan Positions

We have mounted the scanner in a height of approx. 1.40 m on a tripod on top of a movable cart which we use to quickly position the scanner every week on 9 different locations. For positioning the scanner, we rely on rough estimates, yielding only a low precision of about 1 m. However, we use markers for exactly determining the pose of the scanner with respect to these artificial landmarks. Fig. 2 shows the scene as a 3D point cloud, Fig. 4 presents the scan positions, and Fig. 6 shows a point cloud as overlay of all weeks and the correpsonding scanner positions marked by images of the VZ-400 scanner.

C. Marker Placement

Fig. 4 shows the position of the markers as well as the scan locations in a satellite image. From every location, at least three markers are visible that are also visible from adjacent, i.e., previous, locations. The markers consists of special reflectance material and have a diameter of 5 cm. Fig. 5 shows a marker and its appearance in the reflectance image of the scan as well as the points within a point cloud.

D. 3D Scans

We acquired in 14 weeks starting from February 1, 2010, data sets with the 3D laser scanner using a resolution of 0.004° horizontally and vertically, which yields 9001 × 2501 laser shots and thus overall up to 22.5 million laser measurements. Week 1 was a test run with different scanner settings and is not considered in most parts of the data analysis. The VZ-400 uses an unique echo digitization and so-called online waveform processing, which allows the evaluation of multiple target echoes. Up to 7 echoes may be detected, if the laser beam hits several surfaces. Depending on the scanning mode, the number of echoes varies. In the mode "high-speed" multiple echoes occur quite often, while in the mode "high-speed reflector scanning" only targets with high reflectivity are recorded, which lowers the number of multiple echo laser measurements. Fig. 3 presents typical echo distributions. We have chosen the "high-speed reflector scanning" mode for improved marker detection. The scan time needed to complete such a 3D scan is about 3 minutes. Every week we acquired 9 3D scans. 7 laser scans where taken in a loop as seen in Fig. 4. Besides "high-speed" scanning modes, the VZ-400 offers so-called "long-range" operation modes, where a point is measured using several samples and greatly increased scanning times.

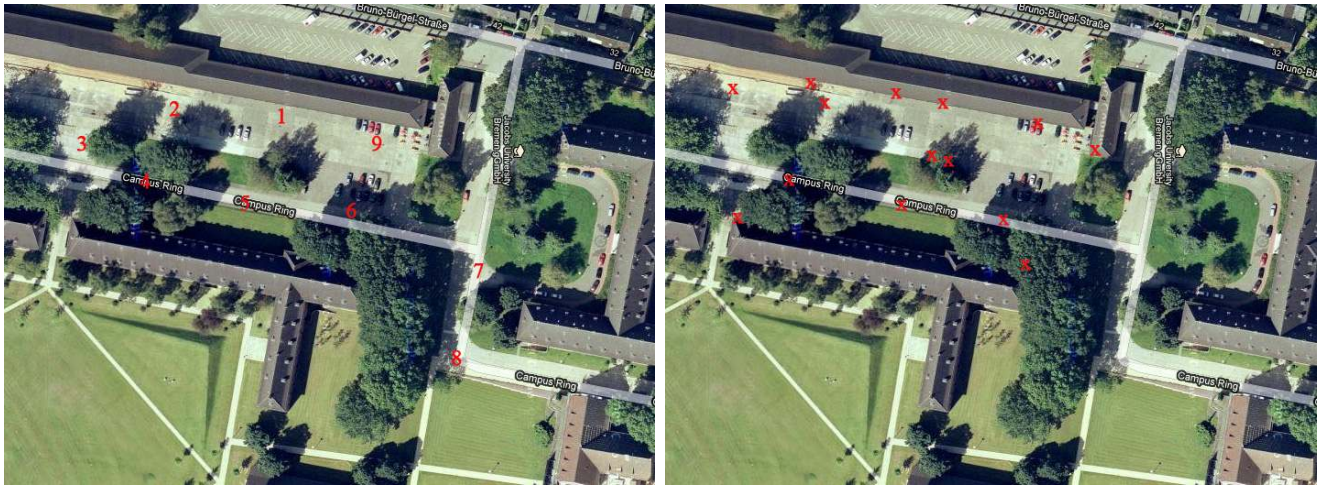

Fig. 4: Satellite image of the test field with scan positions (left) and marker positions (right).

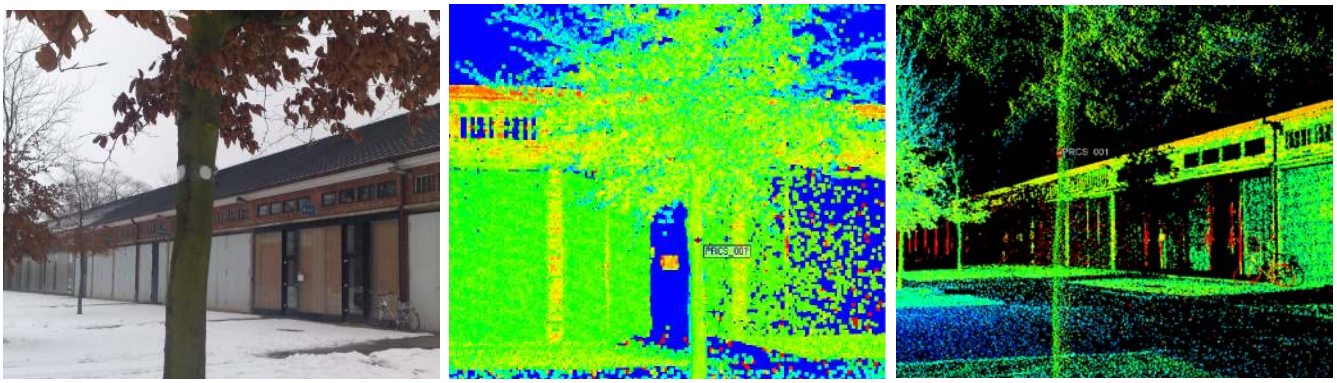

Fig. 5: Left: Marker used in the experiments. Here they are attached to a tree. Middle and right: Marker in the reflectance image of a laser scan and in the corresponding point cloud.

III. 3D MAPPING

Marker based registration uses defined artificial or manually extracted natural landmarks as corresponding points. This manual data association ensures that by minimizing the quadratic error over corresponding points $(\mathbf{m}_i, \mathbf{d}_i)$ in the function

$$E(\mathbf{R}, \mathbf{t}) = \frac{1}{N} \sum_{i=1}^{N} ||\mathbf{m}_i - (\mathbf{R}\mathbf{d}_i + \mathbf{t})||^2 , \qquad (1)$$

leads to a precise transformation, i.e., rotation and translation, $(\mathbf{R}, \mathbf{t})$ that registers the scans in a correct pose. No iterations are required and the above error function can be minimized in closed form in the 2-scan case. Four algorithms are currently known that minimize Eq. (1) in closed form [10]. A critical issue of marker-based registrations is that due to the usage of a small number of markers, the registration quality is quite low, if the markers cannot be extracted accurately. Fig. 5 shows that only a few 3D points belong to markers and therefore it is hard to extract a precise location. A common way to resolve this issue in surveying science is to use a higher resolution scan, in areas, where markers have been detected. This, however is not applicable in our robotic scenario.

Besides manual registration, automatic algorithms are state of the art. Feature based algorithms, like using SIFT features, automatically extract the 3D position of natural features using the remission channel and do not need any iterations nor manual interference for registration [6], [8], [13]. The computational expensive parts of these algorithms is the matching of the features, which has to be verified normally by RANSAC, that slows down computation, too. Point based algorithms, like the iterative closest point (ICP) algorithm [4], register two independently acquired 3D scans or 3D point clouds into a common coordinate system without the need of feature extraction. Here the algorithm relies on minimizing the error function Eq. (1) over closest point correspondences in an iterative fashion given initial pose estimates.

While registering pairwise several 3D data sets using marker and feature-based registration techniques or the ICP algorithm, errors sum up. These errors are due to imprecise measurements and small registration errors. Thus, globally registration algorithms have been developed to reduce these errors. Some of these algorithms, e.g., GraphSLAM algorithms, assume Gaussian distributed errors of the scan poses and find a global minimum [7] while other approaches

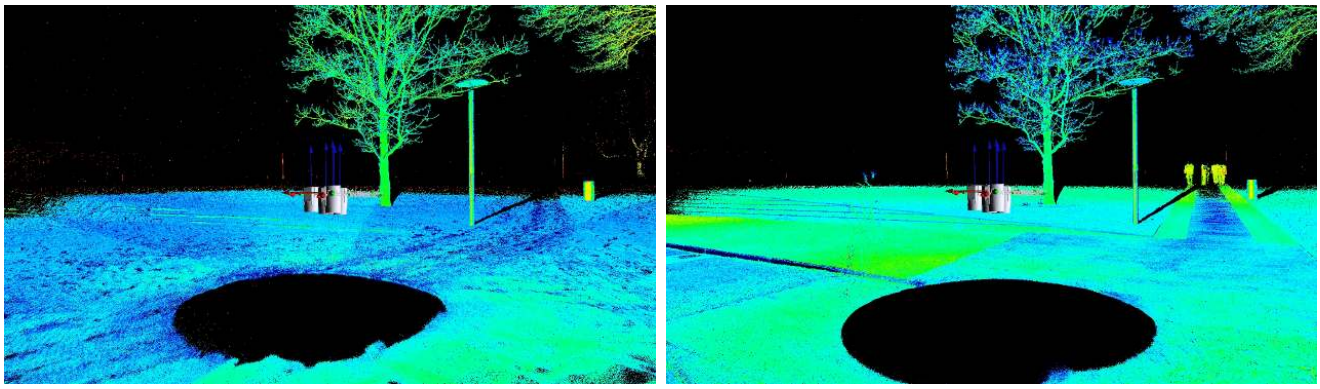

Fig. 6: Marker based registration is used to compute reference scan poses. The scanner depict the scan poses derived by markers. The background is a point cloud acquired in snow. Footprints are clearly visible. Left: 3D scan taken in week 1 (snow), Right: 3D scan taken in week 14.

Fig. 7: Correct registration using SIFT features. The change in the scene does not have an effect on the registration quality.

assume errors in point or feature space and minimize a linearized version of the global error function

$$E(\mathbf{R},\mathbf{t}) = \sum_{(l,k)} \frac{1}{N_{l,k}} \sum_{i=1}^{N_{l,k}} ||\mathbf{R}_l\mathbf{m}_{l,i} + \mathbf{t}_l - (\mathbf{R}_k\mathbf{d}_{k,i} + \mathbf{t}_k)||^2, \quad (2)$$

for all overlapping scan pairs (l,k) and closest point pairs $(\mathbf{m}_{l,i}, \mathbf{d}_{k,i})$. A detailed description of these approaches is given in [12].

The software framework slam6D [1] is used to compute registrations of the laser scans and to analyze the resulting quality. Next, we present our findings:

- Marker based registration of all scans per week was always possible. The overall quality was moderate, due to the small number of markers used. At the loop closure, a small, but noticeable amount of error has been accumulated.
- In addition, we carried out a marker-based registration of all scan positions, i.e., we matched the scan taken at position 1 in week 1 with the scan taken at position 1 in week 2, and so on... In the resulting point clouds changes were clearly visible.

TABLE I: Results of point based registration for all scan positions. Depicted is the difference of distance in cm between a marker in scan 1 and a marker in scan 9 compared to the distance of these two markers in one high resolution scan. The numbers for each scan in the sequence represent the weeks from which the scan has been taken

Scan sequence	Marker	ICP	LUM	ICP+LUM
3, 3, 3, 3, 3, 3, 3	−15.51	51.91	10.42	26.70
3, 4, 3, 3, 4, 3, 4	16.57	25.40	21.65	24.71
3, 4, 6, 8, 10, 12, 14	12.65	73.75	27.85	696.84
3, 3, 3, 4, 4, 4, 4	16.57	−8.33	19.55	8.36
3, 4, 5, 6, 12, 13, 14	12.65	111.59	15.38	384.89
3, 4, 5, 6, 7, 8, 9	−3.94	−36.26	27.20	30.66
3, 14, 3, 3, 14, 3, 14	12.65	3.21	24.99	17.28
3, 3, 3, 14, 14, 14, 14	12.65	4.32	177.53	164.25
3, 3, 3, 5, 5, 5, 5	−0.83	92.60	38.50	75.32
3, 5, 3, 3, 5, 3, 5	−0.83	−4.49	47.07	33.73
3, 11, 3, 3, 11, 3, 11	3.49	64.64	25.75	25.50
3, 3, 3, 11, 11, 11, 11	3.49	55.96	28.45	29.15
3, 9, 10, 11, 12, 13, 14	12.65	−13.34	22.44	−2.54

- We employed feature-based matching to register the 3D scans. For this purpose the popular SIFT method [11] for extraction of robust scale invariant image features is used with an existing open source implementation [2]. In addition, the matching process also takes into consideration the depth at each feature point, obtained by the time-of-flight information for each point, which is used with a RANSAC filtering algorithm [9] to eliminate the outliers. The filtering algorithm is essential in this case, since the number of extracted features, that is around 10,000 for the used 1440×400 images, is large and the number of outliers is also relatively large.
  Table II presents the scan matching results. Surprisingly, basically all scans pairs were matchable, only week 3 and 4 show difficulties. Fig. 7 shows a correct matching result using SIFT features. The features corresponding to the cars do not match or wrong matches are eliminated by RANSAC.
- When trying to register all scans per week the sift method failed due to the small amount of overlap (cf. Fig. 2) in the scans. The repeating structure of the garages on one side of the scene adds further difficulty (cf. Fig 5).

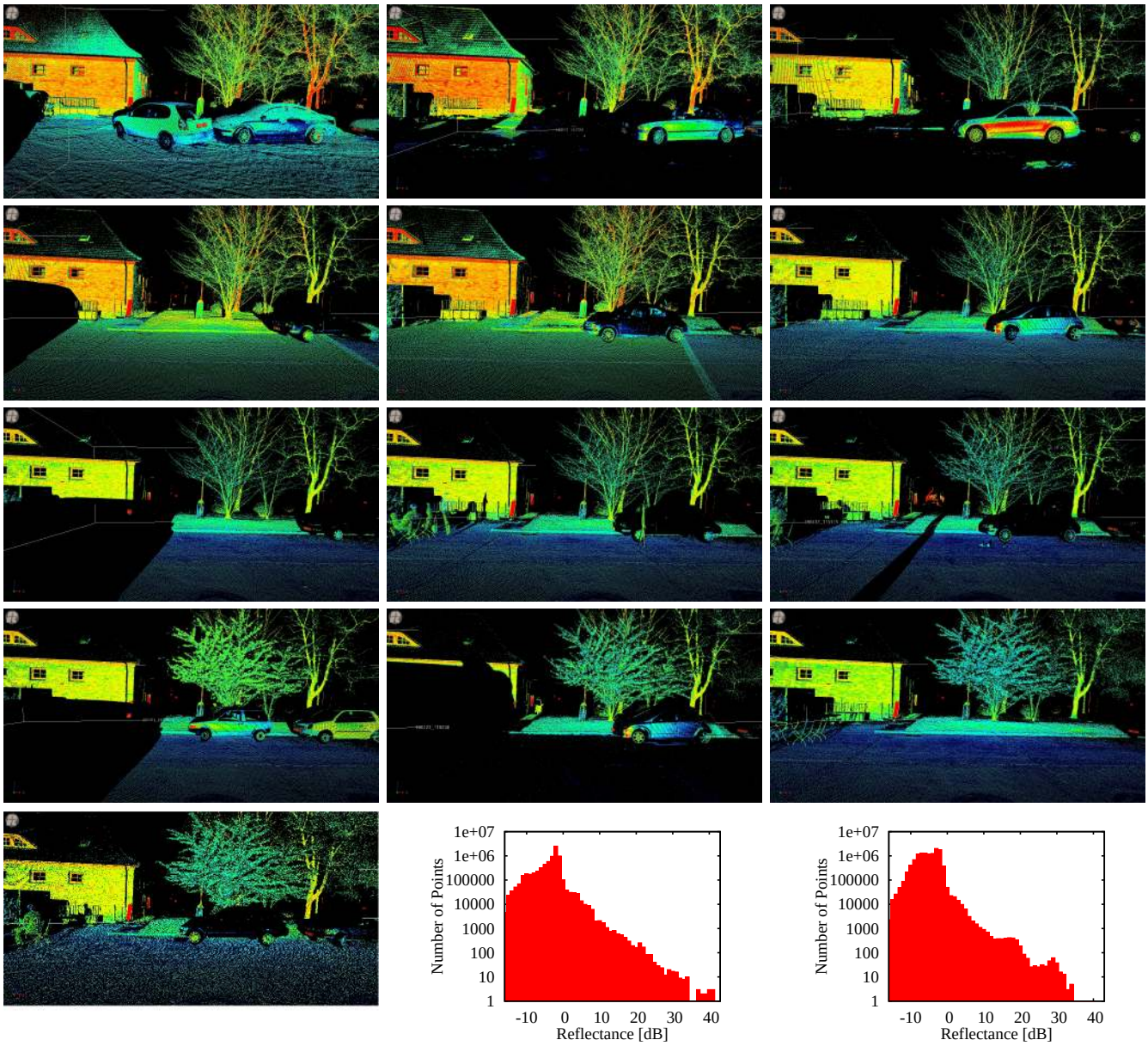

Fig. 8: Changes of the scene during 13 weeks of scanning. The colors represent the reflectance values of the laser beams. The last to images show the reflectance distribution of two scans. First, distribution shifted to the right. Second, distribution without rain

- Initial pose guesses are necessary to register scans on a scan point basis, i.e., without feature extraction. To this end one can either generate such guesses manually or use marker or feature-based methods. ICP and global relaxation produce highly accurate 3D maps, if the scene is static. Changes, e.g., different cars as depicted in Fig. 7, have full impact on the quality of the scan matching. We applied ICP [4] and a global relaxation (LUM) [7] to the scans. Using the marker based pose estimates for all scans per week and all scans per position showed good results. In some cases global relaxation was able to correct the visible errors from the marker based registration. Sequential ICP showed no improvements with respect to the pose estimates. Table I shows the results when combining scans from different weeks. The distance metric is based on the distance between one marker seen from scan position 1 and one marker seen from scan position 9. The reference distance of 59.91 m is calculated from a single high resolution scan that captures both markers. The results show, that the time between the different scans has no systematic impact on the matching results. The marker based distance has to be considered with care as the manual matching procedure was adapted for each week. In many cases the ninth scan was registered directly against the first scan.

IV. DATA ANALYSIS

To analyze the changes in the scene, we developed a tool that compares two given registered 3D scans, by computing

TABLE II: Results of SIFT based registration for scan position 1. Left: Manually inspected registration results. Correct registrations are marked with ✓, incorrect ones with □ and incorrect ones, which have been detected as not matchable by the algorithm with ×. Right: Weather conditions.

Week	2	3	4	5	6	7	8	9	10	11	12	13	14
1	scanner test only												
2	–	×	×	✓	✓	✓	✓	✓	✓	✓	✓	✓	✓
3	□	–	×	×	×	×	×	×	×	×	×	×	×
4	×	✓	–	×	×	×	×	×	×	×	×	×	×
5	✓	×	×	–	✓	✓	✓	✓	✓	✓	✓	✓	✓
6	✓	×	×	✓	–	✓	✓	✓	✓	✓	✓	✓	✓
7	✓	×	×	✓	✓	–	✓	✓	✓	✓	✓	✓	✓
8	✓	×	×	✓	✓	✓	–	✓	✓	✓	✓	✓	✓
9	✓	×	×	✓	✓	✓	✓	–	✓	✓	✓	✓	✓
10	✓	×	×	✓	✓	✓	✓	✓	–	✓	✓	✓	✓
11	✓	×	×	✓	✓	✓	✓	✓	✓	–	✓	✓	✓
12	✓	×	×	✓	✓	✓	✓	✓	✓	✓	–	✓	✓
13	✓	×	×	✓	✓	✓	✓	✓	✓	✓	✓	–	✓
14	✓	×	×	✓	✓	✓	✓	✓	✓	✓	✓	✓	–

Week	Date	Weather Description
1	04/02/2010	Snow, Foggy and slight rain
2	10/02/2010	Snow
3	17/02/2010	Snow
4	24/02/2010	Snow, Foggy and slight rain
5	03/03/2010	Rain
6	10/03/2010	Fog
7	17/03/2010	Cloudy
8	24/03/2010	Cloudy
9	31/03/2010	Rain
10	07/04/2010	Cloudy
11	14/04/2010	Sunny
12	21/04/2010	Rain, Hailstorms
13	28/04/2010	Sunny
14	05/05/2010	Sunny

Fig. 9: Tree-cut. Top: Man in the tree. Bottom: removed branches.

so-called difference scans. Given the scans $A = a_{1,\ldots,N_a} \in \mathbb{R}^3$ and $B = b_{1,\ldots,N_b} \in \mathbb{R}^3$ in a common coordinate frame, we compute those points C that do not have a nearest neighbor within a close limit d, i.e., $C = \{a_i | i \in [1,\ldots,N_a],\ \exists b \in B,\ ||a_i - b|| \leq d\}$. Please note that this operation is not commutative.

A. Temporal Changes

We analyzed the 3D scans to see the effect of temporal changes. Fig. 8 presents a partial view of the scene and the changes within 13 weeks. Clearly, the parking cars change their locations, but some parkers prefer their slot. The first image contains snow on the ground, with footprints etc. In weeks, where no points are on the ground, the ground was either covered by ice or water. These two materials reflect the laser and no point can be measured. In addition, one can see the tree beginning to bloom.

In Fig. 8 the points are colored according to their reflectivity, i.e., the amount of light returned to the scanner. The colors change noticeably due to different environment conditions. The last two images show typical reflectance distributions. Overall, distributions look very similar in all weeks, but during rain or hailstorm the distributions are shifted to the right. In addition, we noticed a shorter average range during these weather conditions. In Fig. 6 these different maximal viewing distances can be seen.

B. Tree Pruning

Typical slow changes occur in the scene where vegetation is present. The acquisition of the data set was chosen, such that we observe winter, where trees have shed their leaves to spring, where they regrow. Fig. 8 shows an example. In addition to the changing foliage, we observed a tree-cut. Each year gardeners prune trees for various reasons. Dead branches are cut off. Low branches are removed to allow safe passage of pedestrians and vehicles underneath.

Fig. 10 presents one tree and the changes before and after the trees have been pruned. It is easy to see that the branches at the log have been cut for esthetic reasons and the others for safety. The same procedure is applicable to observe tree damage after a storm.

V. CONCLUSIONS AND FUTURE WORKS

In this paper we have evaluated the Riegl VZ-400 laser scanner for long term robotic mapping and monitoring applications. The results from our experiments can be summarized as follows:

- The used Riegl laser scanner is generally a well suited sensor for mobile robots. It operates well under normal working conditions, but shows problems with icy and wet surfaces. Therefore, it should be used in fusion with other sensors for critical tasks like drivable surface detection.

Fig. 10: Tree-cut. The brown points are the branches that have been pruned by the gardeners (see Fig. 9).

Fig. 11: The robot Irma3D.

- Manual marker based registration of laser scans is a tedious task. To achieve accurate results the markers need to be clearly visible in neighboring scans. The registration is only applicable for offline tasks and not desirable for large scenes due to the time needed for registration.
- Automatic SIFT based registration of 3D scans works well even is there are some dynamics in the scene given a sufficient amount of overlap. Feature-less approaches have less registration accuracy when the scene is changing and depend on initial pose guesses. To conclude, we recommend using point based registration to produce high accurate maps, if the data is mostly static, i.e., it has been collected in a short time frame or the dynamics in the scene are minor, i.e., mostly buildings. Feature based algorithms, are the method of choice, when change is present.
- Changes in the scene can be easily detected and inspected using a 3D laser scanner. Changes in the geometry are detectable through the measuring principle, while the influence of daylight is less important compared to digital cameras. Weather conditions, however influence scanning as well.

Based on these results, we aim at developing a registration method, that explicitly considers the capturing time, when joining 3D scans.

In addition, we plan to use the Riegl VZ-400 as sensor for the robot Irma3D (Intelligent robot for mapping applications in 3D), see Fig. 11, and to automate surveying and monitoring tasks. Furthermore, we aim at developing an automatic method, for constructing consistent models from a continuously rotating 3D laser scanner on a moving robot.

VI. ACKNOWLEDGMENTS

We acknowledge the work of Darko Makreshanksi, who developed the SIFT based registration for 6D SLAM.

REFERENCES

[1] 6D SLAM – Simultaneous Localization and Mapping with 6 Degrees of Freedom. `http://slam6d.sourceforge.net/`, 2010.
[2] autopano-sift-C. `http://hugin.sourceforge.net/`, 2010.
[3] E. Baltsavias. Airborne Laser Scanning: Existing Systems and Firms and other Resources. *ISPRS Journal*, 54(2-3):164–198, 1999.
[4] P. Besl and N. McKay. A Method for Registration of 3–D Shapes. *IEEE Trans. Patt. Anal. Machine Intell.* , 14(2):239 – 256, 1992.
[5] F. Blais. Review of 20 Years of Range Sensor Development. *Journal of Electronic Imaging*, 13(1):231–240, 2004.
[6] J. Böhm and S. Becker. Automatic Marker-free Registration of Terrestrial Laser Scans using Reflectance Features. In *Proc. of 8th Conf. on Optical 3D Measurement Techn.*, 338–344, Zurich, Switzerland, 2007.
[7] D. Borrmann, J. Elseberg, K. Lingemann, A. Nüchter, and J. Hertzberg. Globally Consistent 3D Mapping with Scan Matching. *Journ. of Robotics and Auton. Systems (JRAS)*, 56(2):130–142, 2008.
[8] C. Brenner, C. Dold, and N. Ripperda. Coarse Orient. of Terrestrial Laser Scans in Urban Environments. *ISPRS Journal*, 63(1):4–18, 2008.
[9] M. A. Fischler and R. C. Bolles. Random SAmple Consensus: a Paradigm for Model Fitting with Applications to Image Analysis and Automated Cartography. *Comm. of the ACM*, 24(6):381–395, 1981.
[10] A. Lorusso, D. Eggert, and R. Fisher. A Comparison of Four Algorithms for Estimating 3-D Rigid Transformations. In *Proc. of the 4th BMVC*, pages 237 – 246, Birmingham, England, 1995.
[11] D. G. Lowe. Distinctive Image Features from Scale-Invariant Keypoints. *Intern. Journ. of Comp. Vision*, 2004.
[12] A. Nüchter, J. Elseberg, P. Schneider, and D. Paulus. Study of Parameterizations for the Rigid Body Transformations of the Scan Registration Problem. *Journal CVIU*, 2010 (accepted).
[13] K. Pathak, D. Borrmann, J. Elseberg, N. Vaskevicius, A. Birk, and A. Nüchter. Evaluation of the Robustness of Planar-Patches Based 3d-Registration using Marker-based Ground-Truth in an Outdoor Urban Scenario. In *Proc. of IROS*, Taipei, Taiwan, 2010 (accepted).
[14] RIEGL Laser Measurement Systems GmbH, Horn, Austria. `http://www.riegl.com/`, 2010.
[15] C. Valgren and A. J. Lilienthal. Sift, Surf & Seasons: Appearance-based Long-term Localization in Outdoor Environments. *Journ. of Robotics and Auton. Systems (JRAS)*, 58(2):157–165, 2010.
[16] W. Wehmann. Untersuchungen zu geeigneten Feldverfahren zur Überprüfung Terrestrischer Laserscanner. Paper des “Offenen Forums TLS”, published online at `www.laserscanning.org`, 2008.
[17] W. Wehmann, C.van Zyl, H. Kramer, R. Zimmermann, and D. Widiger. Einrichtung eines Prüffeldes zur Genauigkeitsbestimmung von Laserscannern und Untersuchung des Scanners LMS-Z360i der Firma RIEGL in diesem Testfeld. *Zeitschrift für Vermessungswesen*, 132(3):175–180, 2007.